

Received 9 May 2019; revised 17 August 2019; accepted 4 September 2019. Date of publication 18 September 2019; date of current version 30 September 2019.  
The review of this article was arranged by Editor K. Shenai.

Digital Object Identifier 10.1109/JEDS.2019.2941519

# Dynamic Behavior Improvement of Normally-Off p-GaN High-Electron-Mobility Transistor Through a Low-Temperature Microwave Annealing Process

HSIEN-CHIN CHIU<sup>1,2,3</sup> (Senior Member, IEEE), CHIA-HAO LIU<sup>1</sup>, YI-SHENG CHANG<sup>1</sup>,  
HSUAN-LING KAO<sup>1</sup> (Member, IEEE), RONG XUAN<sup>4</sup>, CHIH-WEI HU<sup>4</sup>,  
AND FENG-TSO CHIEN<sup>5</sup> (Member, IEEE)

<sup>1</sup> Department of Electronic Engineering, Chang Gung University, Taoyuan 333, Taiwan  
<sup>2</sup> Department of Radiation Oncology, Chang Gung Memorial Hospital, Taoyuan 333, Taiwan  
<sup>3</sup> College of Engineering, Ming Chi University of Technology, Taipei 243, Taiwan  
<sup>4</sup> Technology Development Department, Episil-Precision Inc., Hsinchu 300, Taiwan  
<sup>5</sup> Department of Electronics Engineering, Feng Chia University, Taichung 407, Taiwan

CORRESPONDING AUTHOR: H.-C. CHIU (e-mail: hcchiu@mail.cgu.edu.tw)

This work was supported by the Ministry of Science and Technology under Grant MOST-107-2218-E-182-010.

**ABSTRACT** The surface morphology optimization of ohmic contacts and the Mg out-diffusion suppression of normally off p-GaN gate high-electron-mobility transistors (HEMTs) continue to be challenges in the power electronics industry in terms of the high-frequency switching efficiency. In this study, better current density and reliable dynamic behaviors of p-GaN gate HEMTs were obtained simultaneously by adopting low-temperature microwave annealing (MWA) for the first time. Moreover, HEMTs fabricated using MWA have a higher  $I_{ON}/I_{OFF}$  ratio and lower gate leakage current than the HEMTs fabricated using rapid thermal annealing. Due to the local heating effect, a direct path for electron flow can be formed between the two-dimensional electron gas and the ohmic metals with low bulges surface. Moreover, the Mg out-diffusion of p-GaN gate layer was also suppressed to maintain good current density and low interface traps.

**INDEX TERMS** Microwave annealing, normally off, p-GaN gate HEMT, dynamic behavior.

## I. INTRODUCTION

GaN-based normally-off HEMT with a p-GaN gate structure was implemented to demonstrate single-chip solutions for high-efficiency and compact power conversion systems [1], [3]. For system safety and high efficiency, high-power converters require GaN power devices with low drain lag at high voltages, high robustness, and low leakage current during the off state operation. The high Mg-doped p-type GaN layer could lift the conduction band in the channel at equilibrium due to the thin (12–14 nm) AlGaN barrier layer design, thus realizing the normally off operation. However, based on previous studies, there are two major challenges that dominate the reliability and dynamic behavior of p-GaN gate HEMTs after the high-temperature annealing process.

First, the Ga out-diffusion from a thin AlGaN barrier and the Au interdiffusion of ohmic contact metals caused electrical characteristic degradation [4]. Second, the out-diffusion of Mg into the p-GaN layers results in a low energy level ( $E_C = -3.93$  eV). This result is correlated with the Mg residual compensating impurities [5]–[6]. In this study, we overcame these drawbacks of the traditional p-GaN gate HEMT by adopting a low-temperature microwave annealing (MWA) process together with a p-GaN/AlN/AlGaN/GaN hetero-structure design. The smooth ohmic metal contacts on an AlGaN/GaN heterostructure were obtained by conducting MWA in a low-temperature (450°C–550°C) ohmic contact formation environment. Moreover, based on the measurement results of the secondary ion mass spectrometer (SIMS), the

Mg out-diffusion into the p-GaN/AlN/Al<sub>0.17</sub>Ga<sub>0.83</sub>N/GaN heterostructure beneath the gate metal was also suppressed.

**II. DEVICE STRUCTURE AND FABRICATION**

Figure 1 displays the cross-sectional schematic of the normally off p-GaN/AlN/AlGa<sub>n</sub>/Ga<sub>n</sub> heterostructure HEMT and its corresponding annealing temperature profile in a 2.4-kW microwave power environment. For the proposed p-GaN gate HEMT, the epitaxy wafer was grown by metal-organic chemical vapor deposition on 6-in Si (111) p-type substrates. A 300-nm-thick undoped GaN channel layer was grown on top of a 4-μm-thick unintentionally (UID) AlGa<sub>n</sub>/Ga<sub>n</sub>/AlN buffer layer. A 14-nm-thick undoped composite barrier (1 nm AlN/12 nm Al<sub>0.17</sub>Ga<sub>0.83</sub>N/1 nm Al<sub>0.3</sub>Ga<sub>0.7</sub>N) layer was sandwiched between the Ga<sub>n</sub> channel layer and a 60-nm p-type GaN cap layer. The Mg concentration was 3 × 10<sup>19</sup> cm<sup>-3</sup>, and the active Mg concentration was approximately 1 × 10<sup>18</sup> cm<sup>-3</sup>. This structure exhibited a sheet charge density of 7.2 × 10<sup>12</sup> cm<sup>-2</sup> and a Hall mobility of 1252 cm<sup>2</sup>/V · s at 300 K after removing the p-GaN cap layer. For device fabrication, the active region was protected by a photoresist, and the mesa isolation region was etched to a depth of 200 nm in a reactive ion etching chamber using BCl<sub>3</sub> + Cl<sub>2</sub> mixed gas plasma. The 3-μm-long p-GaN gate island was protected by an SiO<sub>2</sub> passivation layer, and the nongated region was removed by N<sub>2</sub>O oxidation/HCl cyclic wet etching to enable a high etching depth uniformity [7].

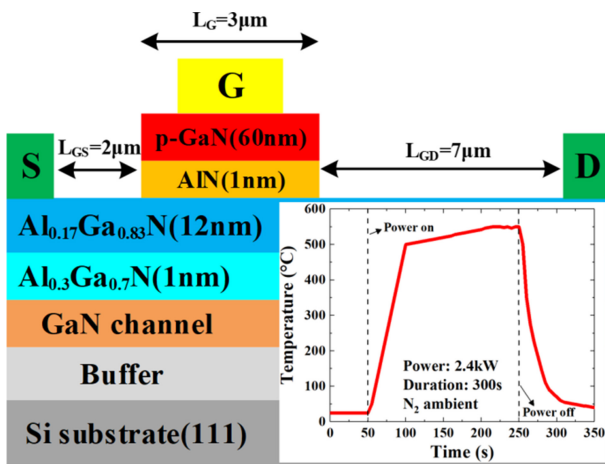


**FIGURE 1.** Cross-sectional schematic of the p-GaN gate HEMT and the temperature profile of the MWA process.

The ohmic contacts were prepared by conducting electron beam evaporation on a multilayer Ti/Al/Ni/Au (25/120/25/150 nm) structure in the traditional lift-off process. For the HEMT fabricated using rapid thermal annealing (RTA-HEMT), the sample was annealed at 875°C for 35 s under nitrogen-rich ambient conditions. For the HEMT fabricated using MWA (MWA-HEMT), the sample was annealed at an RF power of 2.4 kW at a frequency of 6 GHz for 300 s under N<sub>2</sub> atmosphere. The temperature profile of the

MWA process was increased to the temperature range of 450°C–550°C after switching on the 2.4-kW RF power, and the duration of the process was approximately 150 s. The 2-μm-long gate electrode was formed by e-beam evaporation and lift-off of the Ni/Au metal stack. The fabricated devices have a gate width of 50 μm, a gate length of 3 μm, a source–gate distance of 2 μm, and a gate–drain distance of 7 μm. In general, the p-type doped GaN layer should have a flat and uniform Mg profile with a relatively high Mg concentration to obtain a uniform threshold voltage (V<sub>TH</sub>) across the 6-in wafer. However, during the ohmic metal annealing process, Mg diffuses out into the AlGa<sub>n</sub> barrier layer and Ga<sub>n</sub> channel. The Mg concentration as a function of depth beneath the gate metal of the HEMT without annealing, the MWA-HEMT, and the RTA-HEMT are shown in Fig. 2, as measured by SIMS. Obviously, Fig. 2 suggests that the Mg atoms diffused into the thin AlGa<sub>n</sub> barrier layer and Ga<sub>n</sub> channel after the RTA process, which worsened the carrier density of the two-dimensional gas (2-DEG) for the RTA p-GaN HEMT. In other words, the Mg out-diffusion effect of the p-GaN gate HEMT under ohmic annealing was suppressed by the low-temperature MWA process.

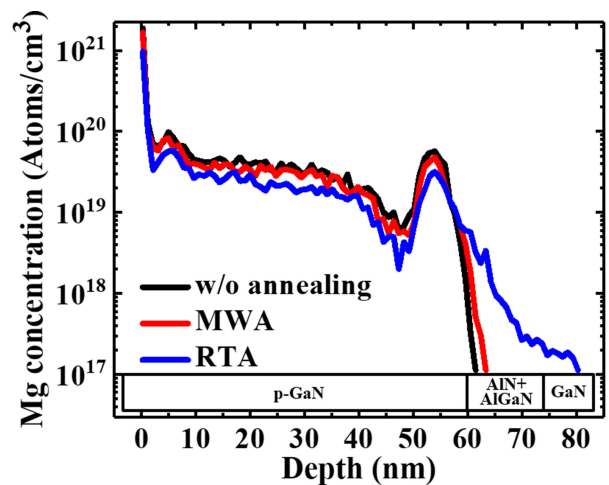


**FIGURE 2.** Mg concentration profiles (SIMS) of the p-GaN gate HEMT fabricated without annealing, by using MWA, and by using RTA.

Figure 3 presents the high-resolution atomic force microscopy (AFM) images and energy dispersive spectrometer (EDS) vertical line scanning analysis for the MWA and RTA p-GaN HEMT. The AFM and EDS were both performed on the source ohmic region directly after annealing processes. By analyzing ohmic contact metal surface AFM images, it was observed that the root mean square roughness was reduced from 32.2 nm (RTA) to 4.67 nm in the AlN/AlGa<sub>n</sub>/Ga<sub>n</sub> heterostructure (nongated region) when the traditional RTA process was replaced with the MWA process. Voids and bulges were caused by the ohmic contact intermetallic compounds under an 875°C RTA environment. Among the deposited ohmic metals, Ti and Al layers are essential as they participate in the reaction with nitrides at the interface and form Ti–N and Al–N [8]. This reaction

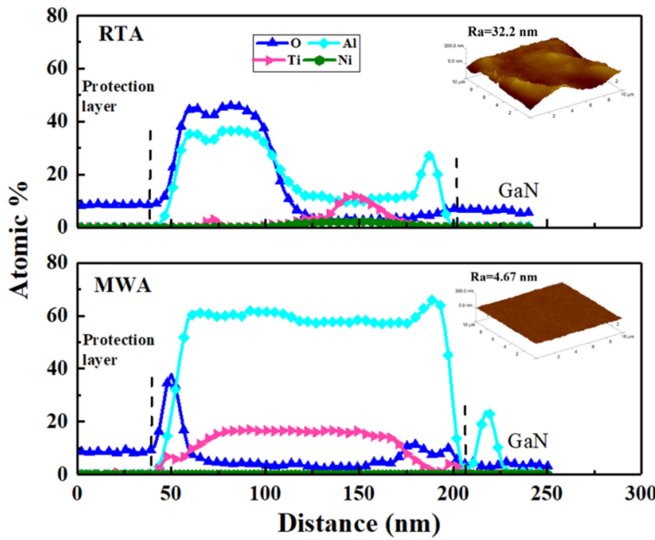


**FIGURE 3.** AFM image and EDS line scan of ohmic contacts in the (a) RTA-HEMTs and (b) MWA-HEMTs.

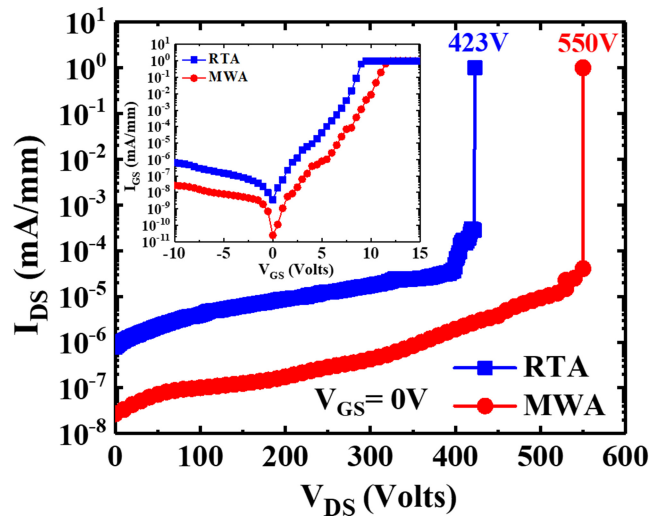
causes an extraction of N atoms from the AlGaN and GaN layers and generates N-vacancies that act as n-type dopants and create a highly doped layer underneath the metallization. Nevertheless, based on the EDS line scan results of the RTA-HEMT, a small quantity of oxygen atoms were driven into the ohmic metal surface to react with Al, thus forming the  $\text{AlO}_x$  compounds at  $875^\circ\text{C}$ . Moreover, the traditional aggregation of Ni–Al for ohmic contact alloys was also observed, and the balling-up of ohmic contacts in the RTA-HEMT was primarily due to the Ni–Al intermetallic compounds and  $\text{AlO}_x$  on the surface. By contrast, the Ti and Al atom distributions are still uniform and flat for ohmic metals of the MWA-HEMT. This behavior is beneficial for improving the ohmic contact resistivity, surface roughness, and potential reliability [9].

In the RTA process, thermal energy is generated using halogen lamps, and the hottest region is near the lamps due to the temperature gradient. Nitrogen and extremely small amounts of oxygen absorb a substantial proportion of the thermal energy in the chamber. In the MWA process, the semiconductor heats up, and the materials are caused to conduct by generating a rapidly changing electromagnetic field that can induce electric current and then cause resistive heating. In another words, the local heating effect occurs on the surface of the epiwafer instead of the environment balanced heating effect. Most of the electromagnetic energy is absorbed by metal pads and semiconductors and converted to electrodynamic energy. Once the microwave is switched-off, the heat on the surface of the metals and semiconductors can be dissipated rapidly to avoid Al oxidation and Ni–Al intermetallic compounds. The contact resistance values of the RTA-HEMT and MWA-HEMT were  $1.15 \times 10^{-6}$  and  $1.01 \times 10^{-6} \Omega\cdot\text{cm}^2$ , respectively. The corresponding channel sheet resistance values were 536 and

452  $\Omega/\square$ , respectively, which were measured using a TLM test structure after annealing.

### III. DEVICE PERFORMANCE AND DISCUSSION

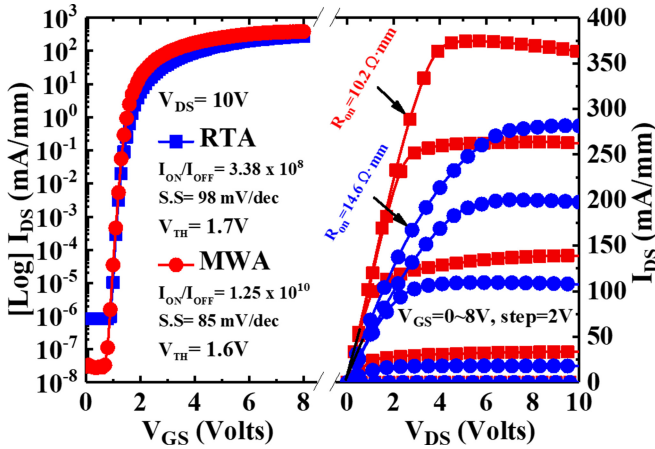
To investigate the improvement in the electrical characteristics of the low-temperature microwave annealing process,  $V_{\text{GS}}-I_{\text{GS}}$  characteristic and the three-terminal off-state breakdown voltage ( $V_{\text{BR}}$ ) curves of both HEMTs were obtained. When these two devices are switched-off, the drain leakage current is almost identical to the gate leakage current, thus indicating that the off-state drain current is mainly attributed to gate leakage. The inset figure in Fig. 4 depicts that the gate leakage current of the MWA-HEMT was around two orders of magnitude lower than that of the RTA-HEMT. The suspected cause of this result is that the MWA process can efficiently suppress the Mg out-diffusion-induced leakage current [5]. A lower gate leakage current of the MWA-HEMT leads to a higher  $V_{\text{ON}}$ . The high  $V_{\text{ON}}$  is beneficial for improving the gate voltage swing range and driver voltage dynamic range. The measured off-state breakdown voltage ( $V_{\text{GS}} = 0 \text{ V}$ ) of the RTA-HEMT was 423 V, and this value was further increased to 550 V by adopting the MWA process.



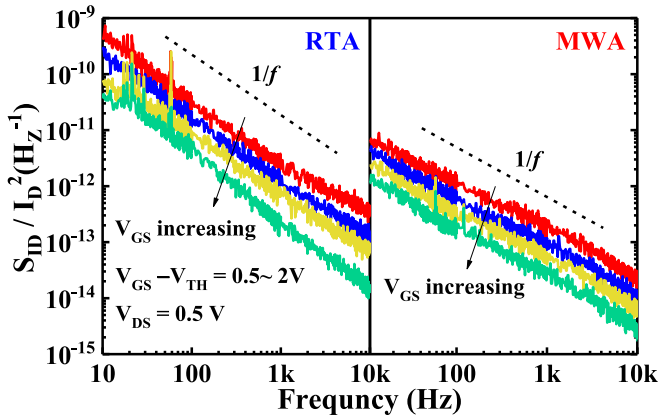
**FIGURE 4.**  $I_{\text{GS}}-V_{\text{GS}}$  and off-state breakdown voltage measurement of the MWA- and RTA- HEMTs.

Figure 5 displays the log-scale  $I_{\text{DS}}-V_{\text{GS}}$  transfer characteristics and  $I_{\text{DS}}-V_{\text{DS}}$  outputs of both devices at a  $V_{\text{DS}}$  value of 10 V. The  $V_{\text{TH}}$  values of the RTA-HEMT and the MWA-HEMT were 1.7 and 1.6 V (defined by  $I_{\text{DS}} = 1\text{mA}/\text{mm}$ ), respectively. The corresponding maximum drain current density ( $I_{\text{Dmax}}$ ) values were 272 and 363 mA/mm, respectively. The  $I_{\text{Dmax}}$  value of the MWA-HEMT was 25% higher than that of the RTA-HEMT because the Mg out-diffusion was suppressed so that the 2-DEG carrier density was maintained. Thus, the static  $R_{\text{on}}$  value of the MWA-HEMT was improved to  $10.2 \Omega\cdot\text{mm}$  which corresponds to a specific on-resistance ( $R_{\text{on}} \cdot A$ ) of  $1.32 \text{ m}\Omega\cdot\text{cm}^2$  at a  $V_{\text{GS}}$  value of 8 V. These values of the RTA-HEMT were  $14.6 \Omega\cdot\text{mm}$

and  $1.9 \text{ m}\Omega \cdot \text{cm}^2$ , respectively. For the MWA-HEMT, the reduction in the off-state  $I_{DS}$  leakage current increased the magnitude of the on/off drain current ratio by approximately two orders of magnitude. The subthreshold swing slope (SS) of the MWA-HEMT was improved from 98 to 85 mV/dec compared with that of the RTA-HEMT.



**FIGURE 5.** Log-scale  $I_{DS}$ - $V_{GS}$  transfer and  $I_{DS}$ - $V_{DS}$  output characteristics of the MWA- and RTA-HEMTs.



**FIGURE 6.** LFN spectra characteristics for both devices with various  $V_{GS}$  values.

To further study the Mg out-diffusion-induced traps in the channel layer for both HEMTs, low-frequency noise (LFN) spectra with various gate overdrive bias voltages ( $V_{GS}-V_{TH}$ ) were measured, as presented in Fig. 6. The on-wafer  $1/f$  noise in the 10–10 kHz frequency range was measured using a noise analyzer (Agilent 35670A) and  $1/f$  noise measurement system software. Obviously, the noise spectra are lower in MWA-HEMT at the  $V_{GS}-V_{TH}$  of 0.5~2 V range. The slopes of the  $S_{ID}/I_D^2$  versus  $V_{GS}-V_{TH}$  were also calculated for both devices and these values were  $-1.4$  and  $-1.3$  for the MWA and RTA devices, respectively. If the slope is close to  $-1$ , then the spectral fluctuation is dominated by the mobility fluctuation model, but if it approaches  $-2$ , it is dominated by fluctuation in the carrier numbers [10]. A value between  $-1$

**TABLE 1.** Summary of HOOGE's constant with various gate voltage overdrives of RTA-HEMTs and MWA-HEMTs.

Hooge's constant, $\alpha_H$				
$V_{GS}-V_{TH}$	0.5V	1V	1.5V	2V
RTA	$5.23 \times 10^{-3}$	$5.9 \times 10^{-3}$	$3.29 \times 10^{-3}$	$3.64 \times 10^{-3}$
MWA	$2.3 \times 10^{-4}$	$2.27 \times 10^{-4}$	$2.15 \times 10^{-4}$	$1.1 \times 10^{-4}$

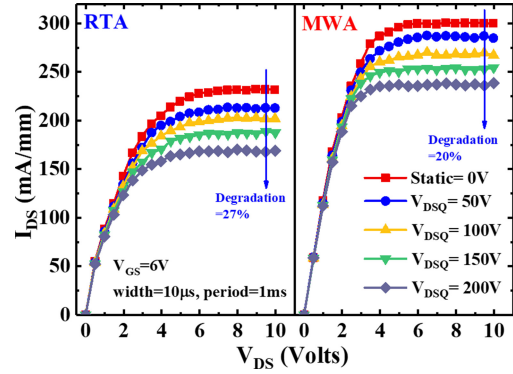


**FIGURE 7.** Pulsed  $I_{DS}$ - $V_{DS}$  characteristics at the quiescent gate bias ( $V_{GSQ}$ ) point of 0 V with a pulse width of  $10 \mu\text{s}$  and pulse period of 1 ms. Subsequently, the quiescent drain bias ( $V_{DSQ}$ ) was swept from 0 to 200 V (in 50 V increments).

and  $-2$  indicates that the noise is attributable to the correlation between the number of carriers and mobility fluctuation. Therefore, the mobility fluctuation associated with Mg out-diffusion-induced traps dominates the low frequency noise in this case. The results also showed the highly agreement to the device  $R_{on}$  and sheet resistivity. In addition, if the mobility fluctuation model was verified in device low frequency noise phenomenon, then the so-called Hooge parameter can be extracted as an intuitive index.

Here,  $\alpha_H$  can provide a measure of the total number of active traps, which cause noise; can be used as a rough figure of merit to characterize these devices; and can be expressed by the following equation [10]–[13]:

$$S_{ID}/I_D^2 = \frac{\alpha_H q}{f W L C_i |V_{GS} - V_{th}|} \quad (1)$$

where  $f$  is the frequency,  $C_i$  is the unit capacitance of the gate insulator,  $q$  is the elementary electron charge. Table 1 summarizes Hooge's constant with various gate voltage overdrives for both devices. The  $\alpha_H$  value of the MWA-HEMT was on the order of  $10^{-4}$  and of the RTA-HEMT was on the order of  $10^{-3}$ . The evidence clearly suggests the suppression of the Mg out-diffusion-induced trap centers occur at the AlN/AlGaIn/GaN interface in the MWA-HEMT. Figure 7 displays the pulsed I-V characteristics of both devices that were switched on from the off state with a  $V_{GSQ}$  of 0 V, the  $V_{DSQ}$  value ranging from 0 to 200 V, a voltage step of 50 V at room temperature, and an on-state gate bias of 6 V [11]. The device was switched on with a pulse width of  $1 \mu\text{s}$  and a pulse period of  $10 \mu\text{s}$ . Clearly, the degradation

in  $I_{DS}$  was improved by approximately 7% in the MWA-HEMT at a  $V_{DS}$  of 10 V. This implied that the channel trap density of the MWA-HEMT was lower than that of the RTA-HEMT. In other words, reducing the Mg concentration up to an Mg level at which the 2-DEG carrier density is no longer strongly influenced by Mg out-diffusion results in a significant reduction in dynamic  $R_{ON}$ . In the case of low Mg concentration, the dynamic behavior is no longer dominated by the Mg out-diffusion consequences, which is the bottleneck of normally off p-GaN HEMTs.

#### IV. CONCLUSION

The MWA method was adopted to form ohmic contacts of a p-GaN gate HEMT. The use of the low-temperature MWA technique resulted in comparatively superior electrical characteristics and a much smoother surface of the MWA-HEMTs than those of RTA-HEMTs. The MWA-HEMT exhibited a leakage current of as low as  $10^{-8}$  mA/mm, which was approximately two orders of magnitude lower than the current exhibited by the RTA-HEMT. An extremely high on/off drain current ratio of up to  $1.25 \times 10^{10}$  was obtained. Moreover, the SIMS analysis indicated that Mg out-diffusion in the conventional RTA method degraded the dynamic behavior of the device. The low-temperature MWA process can suppress Mg out-diffusion beneath the gate and minimize ohmic contact bulges caused by AlOx and Ni-Al intermetallic compounds. The experimental results imply that the MWA technique is a promising method for fabricating high-performance normally off p-GaN HEMTs.

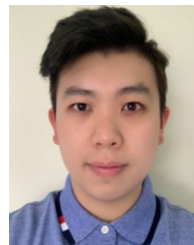
#### REFERENCES

- [1] M. Ishida, T. Ueda, T. Tanaka, and D. Ueda, "GaN on Si technologies for power switching devices," *IEEE Trans. Electron Devices*, vol. 60, no. 10, pp. 3053–3059, Oct. 2013.
- [2] D. Reusch, J. Strydom, and A. Lidow, "A new family of GaN transistors for highly efficient high frequency DC-DC converters," in *Proc. IEEE Appl. Power Electron. Conf. Expo*, Mar. 2015, pp. 1979–1985.
- [3] O. Hilt, F. Brunner, E. Cho, A. Knauer, E. Bahat-Treidel, and J. Würfl, "Normally-off high-voltage p-GaN gate GaN HFET with carbon-doped buffer," in *Proc. IEEE 23rd Int. Symp. Power Semicond. Devices ICs (ISPSD)*, May 2011, pp. 239–242.
- [4] M. Piazza, C. Dua, M. Oualli, E. Morvan, D. Carisetti, and F. Wyczisk, "Degradation of TiAlNiAu as ohmic contact metal for GaN HEMTs," *Microelectron. Rel.*, vol. 49, nos. 9–11, pp. 1222–1225, 2009.
- [5] N. E. Posthuma *et al.*, "Impact of Mg out-diffusion and activation on the p-GaN gate HEMT device performance," in *Proc. IEEE 28th Int. Symp. Power Semicond. Devices ICs (ISPSD)*, Jun. 2016, pp. 95–98.
- [6] A. R. Arehart, A. A. Allerman, and S. A. Ringel, "Electrical characterization of n-type  $Al_{0.3}Ga_{0.7}N$  Schottky diodes," *J. Appl. Phys.*, vol. 109, no. 11, pp. 1–10, Jun. 2011.
- [7] H.-C. Chiu *et al.*, "High-performance normally-off p-GaN gate HEMT with composite  $AlN/Al_{0.17}Ga_{0.83}N/Al_{0.3}Ga_{0.7}N$  barrier layers design" *IEEE J. Electron Devices Soc.*, vol. 6, no. 1, pp. 201–206, Jan. 2018.
- [8] W. Macherzynski *et al.*, "Effect of annealing temperature on the morphology of ohmic contact Ti/Al/Ni/Au to n-AlGaIn/GaN heterostructures," *Optica Applicata*, vol. 39, no. 4, pp. 673–679, 2009.
- [9] Z. Dong *et al.*, "High temperature induced failure in Ti/Al/Ni/Au ohmic contacts on AlGaIn/GaN heterostructure," *Microelectron. Rel.*, vol. 52, no. 2, pp. 434–438, 2012.
- [10] P. Magnone *et al.*, "1/f noise in drain and gate current of MOSFETs with high- $k$  gate stacks," *IEEE Trans. Device Mater. Rel.*, vol. 9, no. 2, pp. 180–189, Jun. 2009.

- [11] O. Jardel *et al.*, "A drain-lag model for AlGaIn/GaN power HEMTs," in *Proc. IEEE MTT-S Int. Microw. Symp.*, 2007, pp. 601–604.
- [12] G. Ghibaudo, O. Roux, C. Nguyen-Duc, F. Balestra, and J. Brini, "Improved analysis of low frequency noise in field-effect MOS transistors," *Physica Status Solidi A*, vol. 124, no. 2, pp. 571–581, 1991.
- [13] M. R. Hasan, A. Motayed, M. S. Fahad, and M. V. Rao, "Fabrication and comparative study of DC and low frequency noise characterization of GaN/AlGaIn based MOS-HEMT and HEMT," *J. Vac. Sci. Technol. B*, vol. 35, no. 5, 2017, Art. no. 052202.



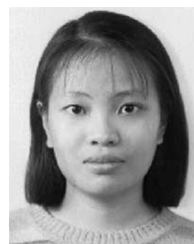
**HSIEN-CHIN CHIU** (S'01–M'02–SM'14) received the Ph.D. degree in electrical engineering from National Central University, Taoyuan, Taiwan, in 2003. He is currently a Professor with the Department of Electronic Engineering, Chang Gung University, Taoyuan, Taiwan, where he has been serving as the Director of High Speed Intelligent Communication Research Center since 2012. He has authored or coauthored over 180 SCI journal publications. His research interests include the microwave, millimeter wave integrated circuits, GaAs, and GaN FETs fabrication and modeling. He was invited to join the publicity and marketing team of Adcom Committees Organization in IEEE Microwave Theory and Techniques Society. He is a member of Phi Tau Phi.



**CHIA-HAO LIU** received the M.S. degree from the Department of Electron Engineering, Chang Gung University, Taoyuan, Taiwan, in 2019, where he is currently pursuing the Ph.D. degree. He is interested in III–V compound semiconductor power devices.



**YI-SHENG CHANG** received the M.S. degree from Asia University, Taichung, Taiwan, in 2014, and the Ph.D. degree from Chang Gung University, Taoyuan, Taiwan, in 2019. His research interest mainly focuses on III–V compound semiconductor power devices.



**HSUAN-LING KAO** received the B.S. degree in electrical engineering from Chang Gung University, Taoyuan, Taiwan, in 1998, and the M.S. and Ph.D. degrees in electronics engineering from National Chiao Tung University, Hsinchu, Taiwan, in 2000 and 2006, respectively. From 2000 to 2006, she was with Macronix Company, Hsinchu. Since October 2006, she has been with the Department of Electronics Engineering, Chang Gung University, where she is currently a Professor. Her current research interests include microwave and millimeter-wave devices and integrated circuits. She is a Technical Reviewer of the IEEE TRANSACTIONS ON INDUSTRIAL ELECTRONICS, IEEE ELECTRON DEVICE LETTERS, the *Transactions on Microwave Theory and Techniques*, and the *International Journal of Electronics*.



**RONG XUAN** was born in Tapei, Taiwan, in 1975. He received the Ph.D. degree in electro-physics from National Chiao Tung University, Taiwan, in 2012.

Since 2002, he has been an Engineer with the Department of Electronic and Optoelectronic Research Laboratories, ITRI, Taiwan. He is currently the Director of the Technology Development and Compound Business Division, Episil-Precision Inc., Taiwan. His research focuses on III-V compound devices, including InGaAsP, AlGaInAs, and

InGaN materials-based edge emitting laser diodes and GaN HEMT.



**FENG-TSO CHIEN** (M'00) was born in Taichung, Taiwan, in 1972. He received the B.S., M.S., and Ph.D. degrees in electrical engineering from National Central University, Taoyuan, Taiwan, in 1994, 1996, and 2000, respectively. Since 2002, he has been a Faculty Member with the Department of Electronic Engineering, Feng Chia University, Taichung. His current research interests include submicrometer technology, thin-film transistors for liquid crystal display, III-V

microwave and millimeter-wave devices, power MOSFETs, insulated-gate bipolar transistors, optoelectronic devices, and integrated circuits.



**CHIH-WEI HU** was born in Taoyuan, Taiwan, in 1974. He received the Ph.D. degree in electronics engineering from National Tsing-Hua University, Taiwan, in 2006. Since 2007, he has been an Engineer with the Department of Electronic and Optoelectronic Research Laboratories, ITRI, Taiwan. He is currently a Project Manager of the Technology Development and Compound Business Division, Episil-Precision Inc., Taiwan. His research focuses on metal organic chemical vapor deposition growth technology on III-V

compound devices, including InGaAsP, AlGaInAs, and InGaN materials-based edge emitting laser diodes, vertical cavity surface emitting laser, InGaAs PIN, and GaN HEMT.